Diamond & Related Materials 59 (2015) 54–61

Contents lists available at ScienceDirect

Diamond & Related Materials

journal homepage: www.elsevier.com/locate/diamond

Imaging of diamond defect sites by electron-beam-induced current

S. Kono [a,*,1], T. Teraji [b], H. Kodama [a], A. Sawabe [a]

[a] Dept. of Electric Engineering and Electronics, Aoyama Gakuin University, Sagamihara 252-5258, Japan
[b] National Institute for Materials Science, 1-1 Namiki, Tsukuba, Ibaraki 305-0044, Japan

ARTICLE INFO

Article history:
Received 23 June 2015
Received in revised form 8 August 2015
Accepted 12 September 2015
Available online 16 September 2015

Keywords:
Diamond
Electron-beam-induced current
Schottky device
Defect

ABSTRACT

The method of electron-beam-induced current (EBIC) was used to visualize the defect sites on a p-type (boron-doped) diamond (001) film. For this purpose, an Ag-Schottky layer (~2 mm × ~2 mm × ~50 nm) was deposited on the oxygen-terminated p-type diamond (001) film and used as a source of EBIC signal. The signal current of EBIC image appeared to be as large as ~1200 times that of the incident electron-beam current and the difference range in image intensity was also large (1–1200). The observed EBIC images showed many kinds of signatures that are possible 'killer' defects for Schottky devices. In order to identify 'killer' defects in the EBIC image, an array of Ag-dots (~40 × ~50 μm^2) was deposited on an oxygen-terminated p-type diamond (001) film and I–V characteristics were measured on 53 Ag-dots. The resulting I–V characteristics showed that 21 Ag-dots reside on 'killer' defects. Comparison between the EBIC image and the positions of Ag-dots residing on 'killer' defects showed that large dark dots in EBIC image correspond to the position of 'killer' defects. The number density of the large dark dots (i.e., 'killer' defects) was ~10^4/cm^2 in the present sample. It is suggested that a high yield Schottky-junction device may be fabricated by avoiding these 'killer' defects by the use of EBIC.

1. Introduction

Diamond is considered to be an ultimate material for durable electronic devices such as high-power/-frequency electronic devices due to its extraordinary properties (high thermal conductivity, mechanical hardness, chemical inertness, high mobilities of electrons and holes, and a high breakdown electric field). For the fabrication of diamond electronic devices, diamond films of p-type and/or n-type and/or non-doped are usually prepared by chemical vapor deposition (CVD) on high pressure and high temperature (HPHT) synthetic diamond crystals. However, perfect (defect-free) HPHT diamond crystals have never been acquired; many kinds of defects are found in HPHT diamond crystals as well as in natural diamond crystals [1]. For the fabrication of CVD diamond films, HPHT or natural diamond crystals with relatively fewer defect densities are cut into desired substrate shapes and the surfaces are polished. Defects in the substrate crystals are usually inherited to the CVD films and additional defects grow-in due to the cutting/polishing processes, and due to doping and CVD growth [2]. In order to reduce the defects caused by CVD growth, special cares are taken some times, in and/or after the process of polishing [3,4].

There are many types of defects and they may be classified into point defects and extended defects [5–7]. The extended defects may be regarded to have fatal effects on diamond electronic devices. The type, the density, and the position of the defects are evaluated by several means, such as the etch-pit method [3,8], X-ray topography [9], and birefringence microscopy [10]. Typical defect densities as found by the etch-pit method on diamond (001) surfaces are ~3 × 10^5/cm^2 and ~3 × 10^6/cm^2 for Ib HPHT and CVD samples, respectively [3]. A defect density of ~2 × 10^5/cm^2 by the etch-pit method is recently reported for a CVD diamond (001) surface on Ib HPHT substrate [11]. Another type of CVD diamond films, i.e., hetero-epitaxial diamond films are reported to have etch-pit defect densities that are far behind the level of CVD diamond films fabricated on HPHT substrate [12]. Typical defect densities as found by X-ray topography vary. They range from ~400/cm^2 [2] for (111) face and ~2000/cm^2 [9] for (100) surface of a IIa type HPHT diamond to ~10^4/cm^2 for (100) face of a CVD and Ib type HPHT diamond [13].

The defects as appeared in the CVD diamond films that are used for devices may be viewed in another way, i.e., 'killer' and 'non-killer' defects where 'killer' defects cause fatal malfunctioning in the electronic device fabricated on the CVD film and 'non-killer' defects cause no malfunctioning. The density of 'killer' defects is, for example, evaluated by Murphy's Eq. from the figure of yield of an actual diamond electronic device [14]. Typical density of 'killer' defects has been reported to be 10^4–10^5/cm^2 for a Schottky junction device fabricated on a Ib type HPHT substrate [15]. A state-of-the-art value of 'killer' defect density on a diamond Schottky-device is reported to be ~600/cm^2 [16].

In the circumstances as described above, it may be useful to find the positions of 'killer' defects before actual device elements are fabricated to avoid the specific 'killer' defects. Recently, Ohmagari et al. [17] reported that a special four-hold pattern in cathodoluminescence (CL) image

* Corresponding author.
E-mail address: kono@tagen.tohoku.ac.jp (S. Kono).
[1] Present status: Visiting researcher, School of Science & Engineering, Waseda University; Professor emeritus of Tohoku University.

http://dx.doi.org/10.1016/j.diamond.2015.09.006
0925-9635/

for 'band-A' emission corresponds to a 'killer' defect. This method was further combined with a local characterization technique of conductive-probe atomic force microscopy [18]. However, in the CL image, there are so many spots of band-A emission and the difference in the shapes of pattern is so subtle that the identification of 'killer' defects seems very difficult. In addition, the defects described in the paper [17] are for the fatal ones inducing large leakage current. In other words, detection of the other kind of killer defects may be difficult by the CL imaging. To the best of the authors' knowledge, there have been no other reports to describe the method of directly locating 'killer' defects. In this paper we report a direct detection method of locating 'killer' defects based on electron-beam-induced current (EBIC). EBIC is commonly used to visualize the depletion regions and further to locate defective sites in semiconductor p–n junctions. EBIC has been applied to diamond crystal p–n junctions to visualize the depletion region [19–21].

In principle, p–n junctions can be replaced by Schottky junctions in EBIC. Application of EBIC to a Au Schottky-junction on a homoepitaxial p-type diamond (001) crystal was reported in 1998 [22]. 10 years later, EBIC was applied to a Pt Schottky-junction on a homoepitaxial p-type diamond (001) crystal [23]. Both studies on the Schottky junction showed that the structures found in EBIC images correspond to the structures found either by optical microscopy (OM) or scanning electron microscopy (SEM), thus, morphological defects such as polishing grooves and shell-shaped cavities were detected by EBIC [22–23]. In this study, we show that EBIC is capable of finding defects that are not obvious by OM and SEM. We further show that EBIC is capable of finding possible 'killer' defects that are not found by OM and SEM. Thus, the map of possible 'killer' defects of a CVD diamond substrate (to be used for device fabrication) can be composed to improve the yield of the device.

2. Scheme of the present EBIC and expected principle

Fig. 1a) shows schematics of the sample used in the present study. An HPHT diamond (100) crystal was used as a substrate and a p-type (boron-doped) diamond layer was deposited by CVD and the surface was oxidized. A silver layer of ~50 nm thick was deposited over the surface except for the periphery. The Ag-layer formed a Schottky-junction to the p-type CVD layer. An EBIC signal line (S) was formed on one corner of the Ag-layer and ohmic contacts (O) were made on several parts of the periphery of the p-type CVD layer. The Ag-layer can in principle cover effectively whole of the p-type layer to find defects on the sample surface. Fig. 1b) shows a schematic energy band diagram at the Schottky junction, where E_V and E_C denote the valence band top and conduction band bottom of the boron-doped diamond, respectively, and E_F denotes the Fermi level. The Schottky barrier height (SBH or ϕ_{SB}) of good Ag Schottky layers on the oxidized diamond (001) surface is determined to be ~1.9 eV [24]. The SBHs at defective sites (possible 'killer' defect sites) are found to be substantially lower [24].

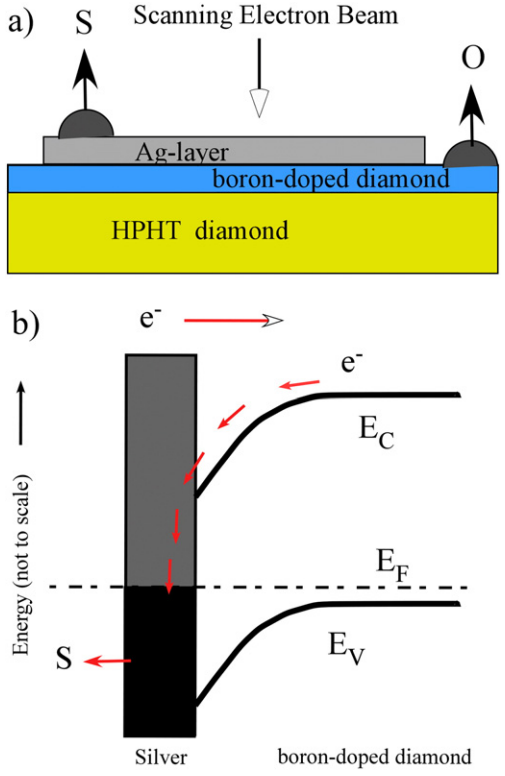

Fig. 1. a) Schematic illustration of the sample used in the present study. b) Schematics of the expected principle of the present EBIC.

For the EBIC measurement, an electron-beam of typically 20 kV is incident on the Ag-layer and scanned over the surface. The penetration depth (diffusion depth) of the electron-beam of 20 kV is expected to be ~4 and ~6 μm in Ag and in diamond, respectively [25], thus sufficient electron intensity is expected in the boron-doped diamond layer and electrons and holes are created in it. Electrons created in the depletion region of the Schottky junction are expected to move through E_C toward the Ag layer, and holes created in the depletion region are expected to move through E_V toward the ohmic contact line O, thus, an EBIC current appears on the signal line S. As will be shown, the EBIC current in the present study is quite large; it is almost 1000 times larger than that of the incident electron-beam current. When the electron-beam is incident on a defective part where SBH is lower, the EBIC current would be less since the potential slope in the depletion region is less steep. It is also possible that a defective part with normal SBH is present but can have an impurity inclusion or other sorts such as carrier traps in the diamond layer. This defective part will cause less effective creation of electrons and holes in the boron-doped layer and/or less effective transfer of electrons and holes toward the respective sides, thus makes less EBIC current. As will be shown, the ratio of EBIC current at a defective part to that of the non-defective part can be as small as ~0.1 and ranges, thus the defective parts are easily recognized and quantified. As will be shown later, the spatial resolution of the present EBIC microscopy is less than 1 μm.

Schottky junction metals other than Ag may also be used in the present EBIC although SBH of Ag junction is one of the largest [24]. In principle, this EBIC method can be applied to n-type diamond samples but the polarity of current would be reversed. Further, a suitable Schottky junction metal must be used. Unfortunately, the properties of Ag Schottky junction on n-type diamonds are not known to the authors' knowledge.

3. Experimental procedure

A commercial (Sumitomo) type-Ib HPHT (001) diamond crystal ($3 \times 3 \times 0.5$ mm^3) was used as a substrate. An additional finer polishing (Syntek) was applied to have an off-angle of ~3° from the surface normal along <110> direction, thus a nominal 3° vicinal (001) surface was created. A boron-doped p-type diamond layer was deposited by microwave-assisted (MW) CVD under the following conditions. Total gas pressure, microwave power, methane concentration (flow ratio of CH_4 to the total gas flow), oxygen concentration (flow ratio of O_2 to the total gas flow), boron concentration (flow ratio of trimethyl boron gas to methane gas), substrate temperature, and duration were 140 Torr, 1.4 kW, 10%, 2%, 4 ppm, 1020 ± 10 °C, and 1 h, respectively. The thickness of the p-type layer was ~3 μm with a boron concentration of ~2×10^{16}/cm^3 as estimated from a low temperature CL spectrum. The sample was then treated in a mixture of nitric and sulfuric acids at 250 °C and rinsed with distilled water; thus, the surface was covered with oxygen. The smoothness (Ra = 0.2–0.3 nm) of the oxygen-terminated surface was confirmed by atomic force microscopy. Micro-Raman spectra were measured on specific places of the oxygen-terminated surface.